

***IN SILICO AND IN VITRO ACTIVITY OF FRIEDELIN N-DERIVATIVES AGAINST PROMASTIGOTE FORMS OF *Leishmania amazonensis****

**Mauro Lúcio Gonçalves de Oliveira<sup>a</sup>, Lucienir Pains Duarte<sup>a</sup>, Grácia Divina de Fátima<sup>a</sup>, Silvia Ribeiro de Souza<sup>b</sup>, Misléia Rodrigues de Aguiar Gomes<sup>b</sup>, Sidney Augusto Vieira-Filho<sup>a,c</sup>, Vera Lucia de Almeida<sup>a,d</sup>,  and Júlio César Dias Lopes<sup>a,\*</sup>, **

<sup>a</sup>Departamento de Química, Instituto de Ciências Exatas (ICEx), Universidade Federal de Minas Gerais, 31270-901 Belo Horizonte – MG, Brasil

<sup>b</sup>Faculdade de Ciências da Saúde, Universidade de Brasília (UnB), Campus Darcy Ribeiro, 70910-900 Brasília – DF, Brasil

<sup>c</sup>Departamento de Farmácia, Universidade Federal de Ouro Preto, Campus Morro do Cruzeiro, 35400-000 Ouro Preto – MG, Brasil

<sup>d</sup>Serviço de Fitoquímica e Prospecção Farmacêutica, Fundação Ezequiel Dias, 30510-010 Belo Horizonte – MG, Brasil

Received: 04/03/2025; accepted: 06/30/2025; published online: 07/22/2025

\*e-mail: jlopes.ufmg@gmail.com

## PART A - OBTENTION AND IDENTIFICATION OF FRIEDELIN N-DERIVATIVES

**Table 1S.** Reaction conditions and yields of N-derivatives **2-4** obtained from friedelin (**1**) isolated from leaves of *Maytenus gonoclada*

N-Derivative	Friedelin ( <b>1</b> ) / mg	Base (quantity)	Solvent	Catalyst	Yield / %
Friedelan-3-(2,4-dinitrophenyl)-hydrazone ( <b>2</b> )	100		EtOH	acetic acid (70 mg)	83
Friedelan-3-oxyme ( <b>3</b> )	100	NOH.HCl (50 mg)	EtOH	pyridine	93
Friedelan-3-hydrazone ( <b>4</b> )	100	N <sub>2</sub> H <sub>4</sub> [5mL (80%) 12 mg]	EtOH	acetic acid	56

The chemical characterization of *N*-derivatives **2**, **3**, and **4** obtained from friedelin (**1**) was carried out through analyses of infrared (IR) and hydrogen and carbon nuclear magnetic resonance (<sup>1</sup>H and <sup>13</sup>C, DEPT-135 (distortionless enhancement by polarization transfer) and 2D NMR) spectral data (Figures 1S to 20S).

Infrared spectra were collected in the range from 4000 to 650 cm<sup>-1</sup> using a PerkinElmer Model Spectrum 2000, equipped with attenuated total reflectance (ATR). <sup>1</sup>H and <sup>13</sup>C NMR spectra were obtained on a Bruker DRX-400 AVANCE spectrometer at 400.22 and 100.63 MHz, respectively. TMS (tetramethylsilane) was used as an internal standard and CDCl<sub>3</sub> or CDCl<sub>3</sub>/pyridine-d<sub>5</sub> as solvent, as indicated in each case.

### Spectral data of friedelan-3-(2,4-dinitrophenylhydrazone) (**2**)

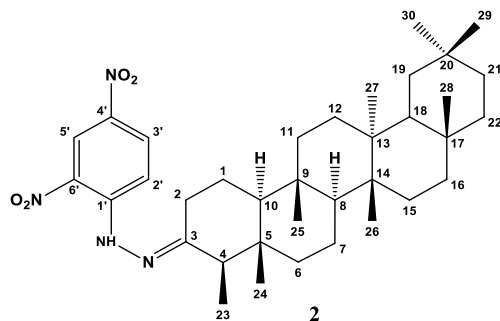


**Figure 1S.** Structure of the friedelan-3-(2,4-dinitrophenylhydrazone) derivative (**2**)

In the infrared spectrum of *N*-derivative **2**, absorption bands were observed at  $3322\text{ cm}^{-1}$  ( $\nu_{\text{NH}}$ ),  $2922\text{ cm}^{-1}$  ( $\nu_{\text{CH}}$ ),  $1621\text{ cm}^{-1}$  ( $\nu_{\text{N}=\text{C}}$ ),  $1588\text{ cm}^{-1}$  ( $\nu_{\text{C}=\text{C}}$ , associated to a double bond of an aromatic group),  $1515\text{ cm}^{-1}$  ( $\text{NO}_2)_n$  ( $n = 2$ ),  $1434$  and  $1390\text{ cm}^{-1}$  ( $\delta_{\text{CH}}$ ) and at  $844\text{ cm}^{-1}$  corresponding to an aromatic carbon bond linked to nitrogen.<sup>1</sup> In the  $^1\text{H}$  NMR spectrum, a quartet was observed at  $\delta_{\text{H}} 2.21$  ( $J 6.0\text{ Hz}$ ), correlated to H-4, which is characteristic of triterpenes of the friedelane series.<sup>2</sup> The multiplet at  $\delta_{\text{H}} 2.94$  was associated with H-12. A singlet was also verified at  $\delta_{\text{H}} 11.25$ , referring to the hydrogen bonded to the nitrogen characteristic of the hydrazone group. Three signals of hydrogen bonded to aromatic carbon at  $\delta_{\text{H}} 7.96$  (d,  $J 10.9\text{ Hz}$ ),  $\delta_{\text{H}} 8.28$  (dd,  $J 2.7$  and  $10.9\text{ Hz}$ ), and  $\delta_{\text{H}} 9.11$  (d,  $J 2.7\text{ Hz}$ ) were correlated with H-2', H-3', and H-5', respectively. In the  $^{13}\text{C}$  NMR spectrum, one signal was detected at  $\delta_{\text{C}} 162.62$ , characteristic of the carbon linked to the hydrazone group, and six signals at  $\delta_{\text{C}} 145.69$ ,  $137.40$ ,  $129.96$ ,  $128.79$ ,  $123.64$  and  $116.45$ , which were attributed to aromatic carbons; C-1'; C-4'; C-5'; C-6'; C-3' and C-2', respectively (Figures 2S to 9S).

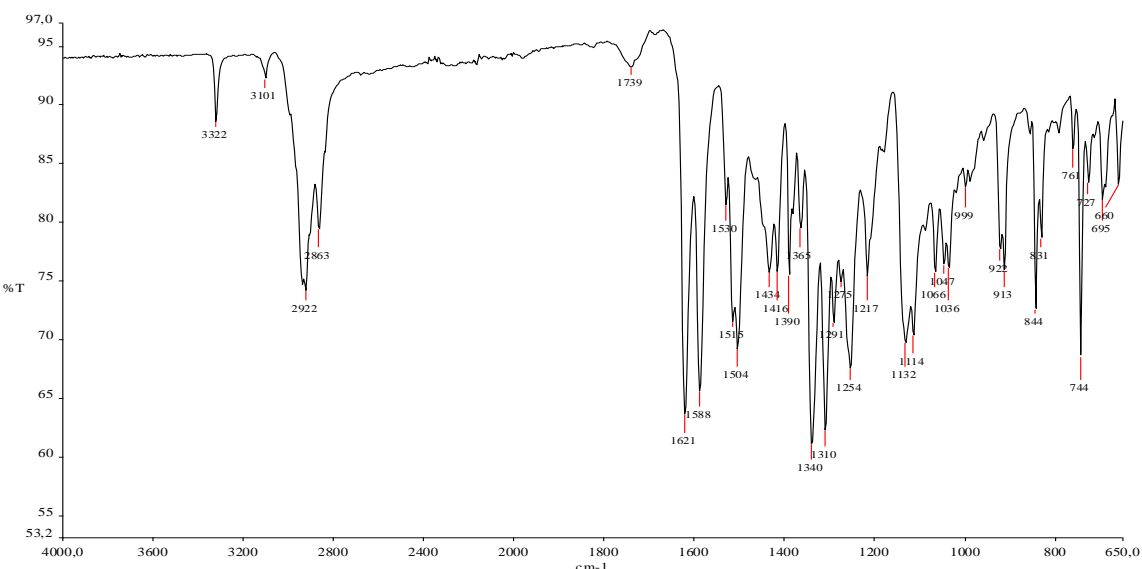


**Figure 2S.** IR spectrum (ATR) of friedelan-3-(2,4-dinitrophenylhydrazone) (2)

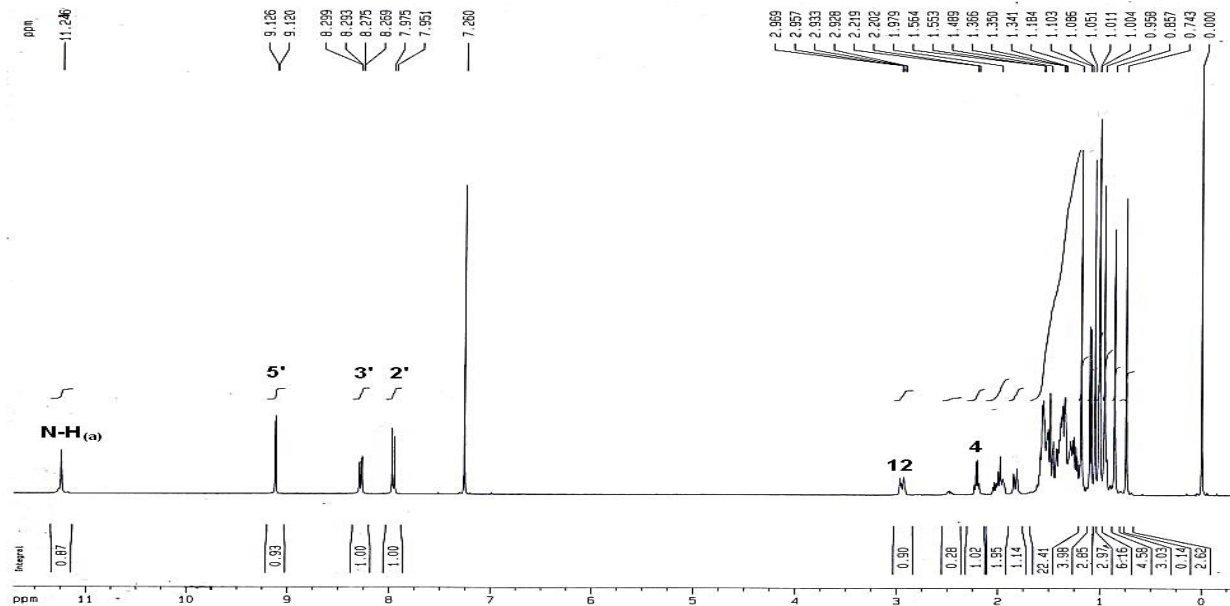


**Figure 3S.**  $^1\text{H}$  NMR spectrum (400 MHz,  $\text{CDCl}_3$ ) of friedelan-3-(2,4-dinitrophenylhydrazone) (**2**)

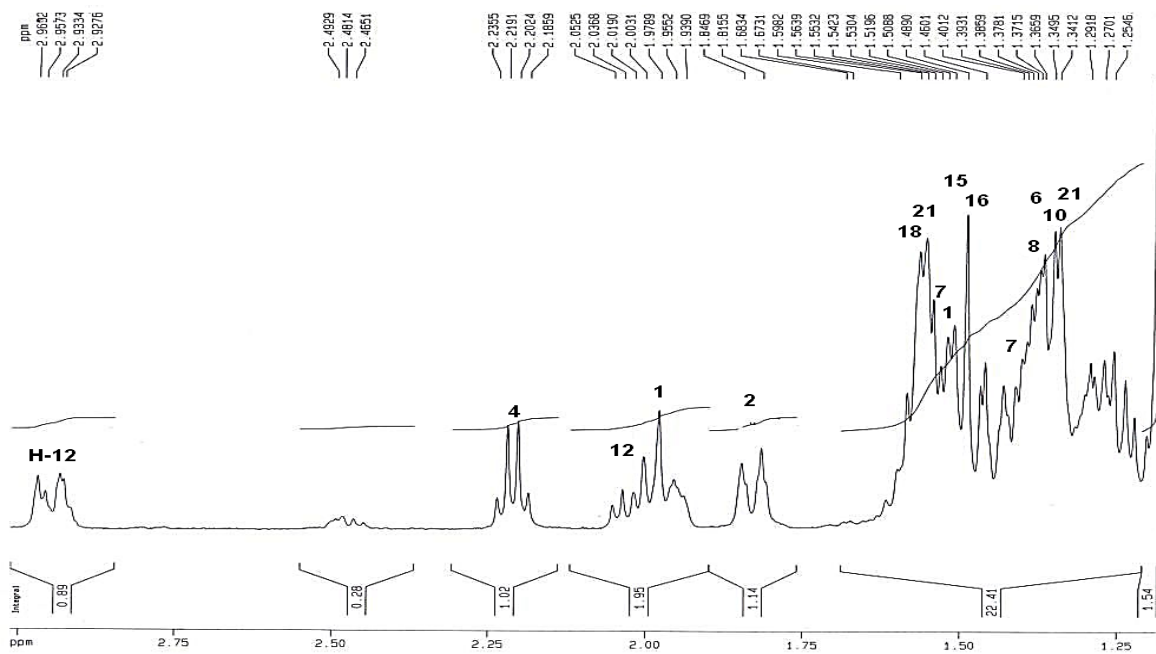


**Figure 4S.**  $^1\text{H}$  NMR spectrum (400 MHz,  $\text{CDCl}_3$ ) of friedelan-3-(2,4-dinitrophenylhydrazone) (**2**). Expansion between  $\delta_{\text{H}}$  1.20 to 3.00 ppm

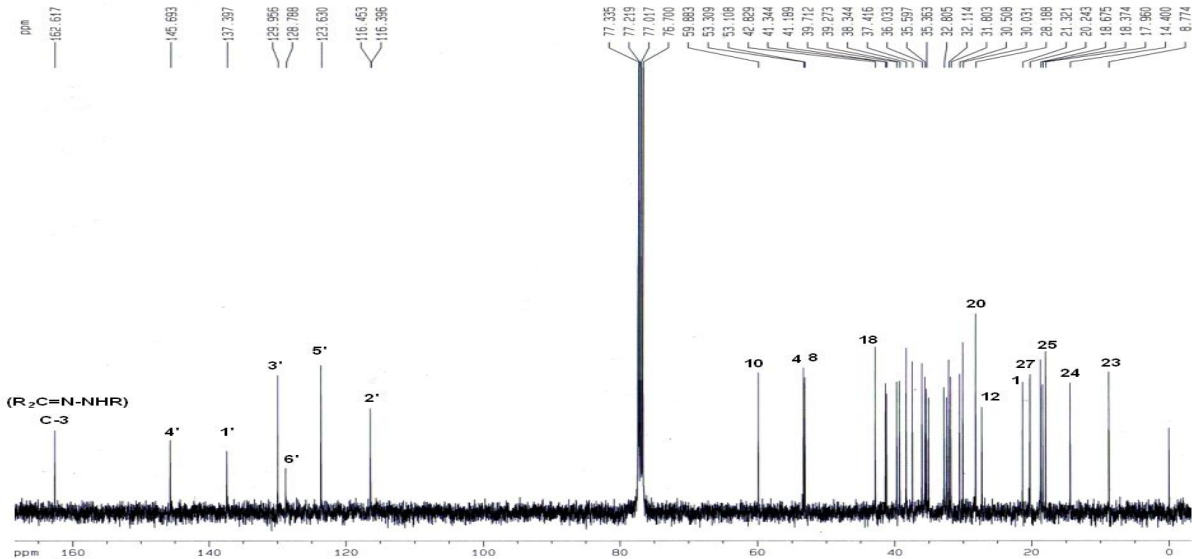


**Figure 5S.**  $^{13}\text{C}$  NMR spectrum (100 MHz,  $\text{CDCl}_3$ ) of friedelan-3-(2,4-dinitrophenylhydrazone) (**2**)

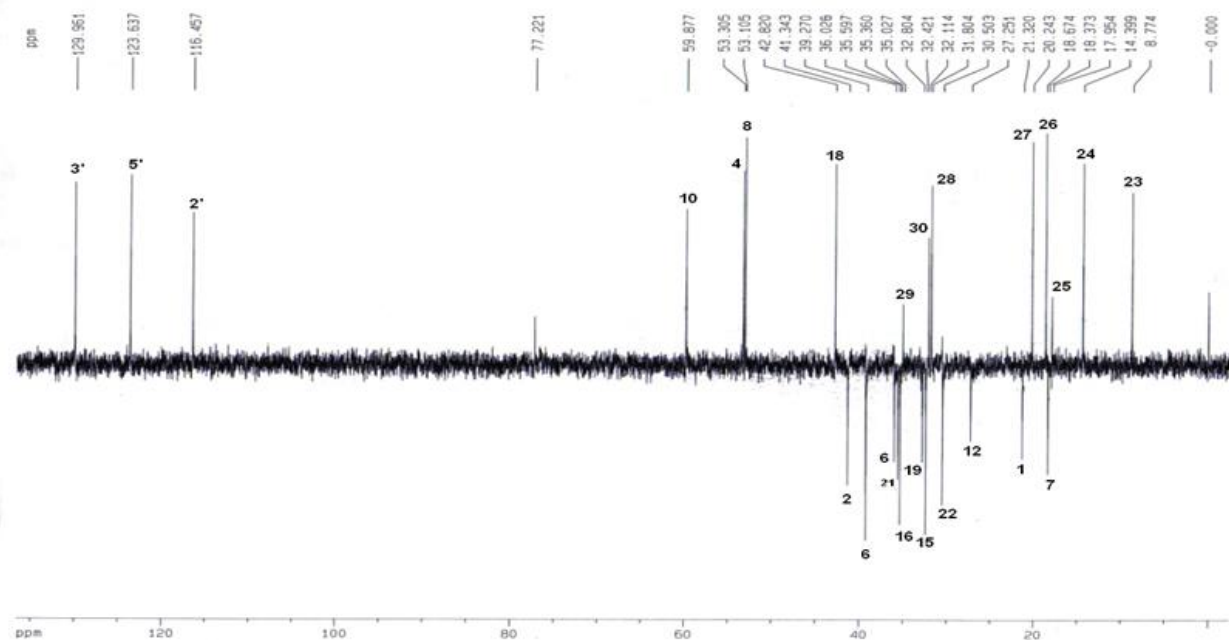


**Figure 6S.** DEPT-135 spectrum (100 MHz,  $\text{CDCl}_3$ ) of friedelan-3-(2,4-dinitrophenylhydrazone) (**2**)

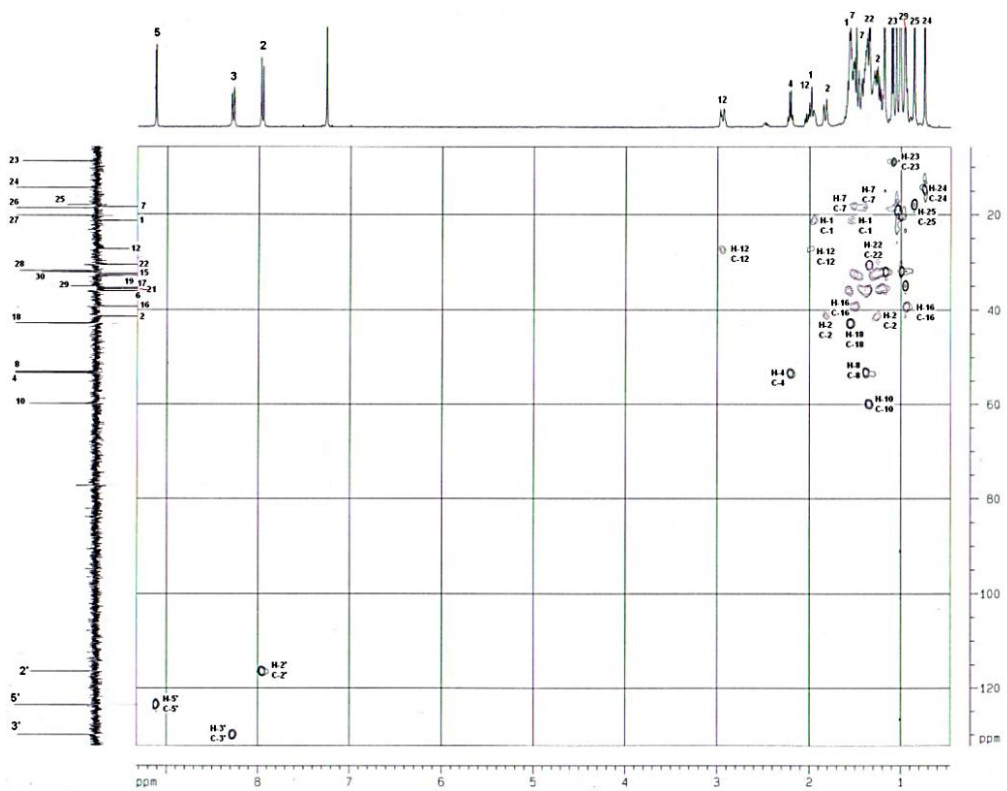


**Figure 7S.** HMQC contour map (400 MHz, CDCl<sub>3</sub>) of friedelan-3-(2,4-dinitrophenylhydrazone) (2)

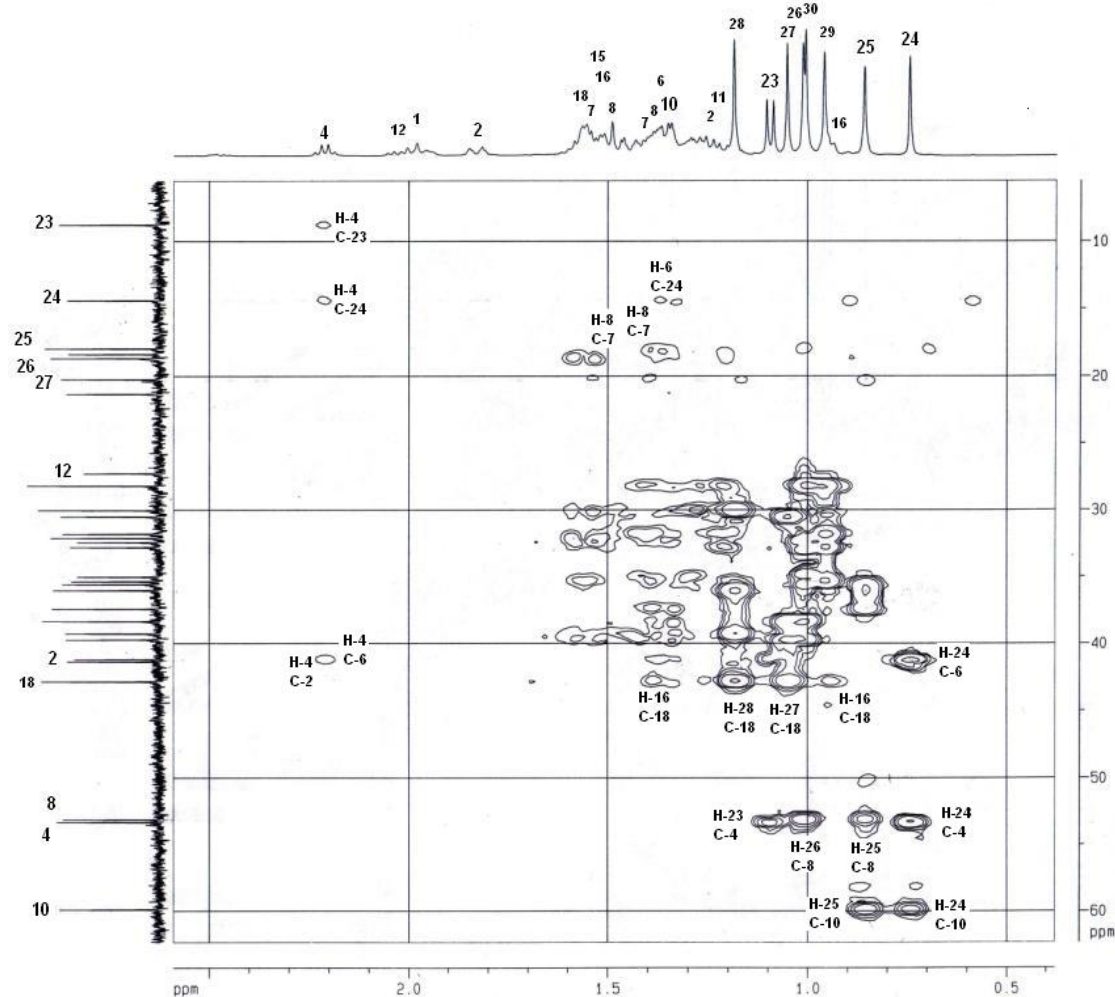


**Figure 8S.** HMBC contour map (400 MHz,  $CDCl_3$ ) of friedelan-3-(2,4-dinitrophenylhydrazone) (2). Expansion between  $\delta_C$  5.00 to 62.00 ppm

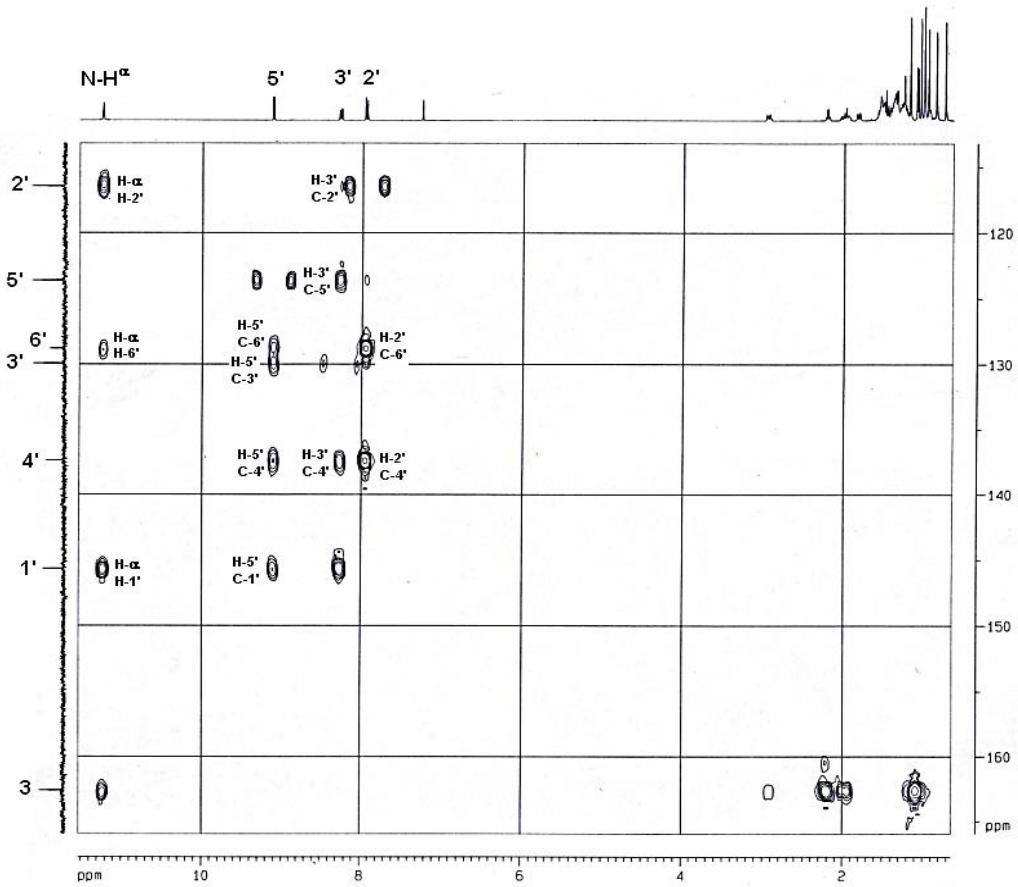


**Figure 9S.** HMBC contour map (400 MHz,  $CDCl_3$ ) of friedelan-3-(2,4-dinitrophenylhydrazone) (2). Expansion between  $\delta_C$  112.50 and 167.00 ppm

### Spectral data of friedelan-3-oxime (3)

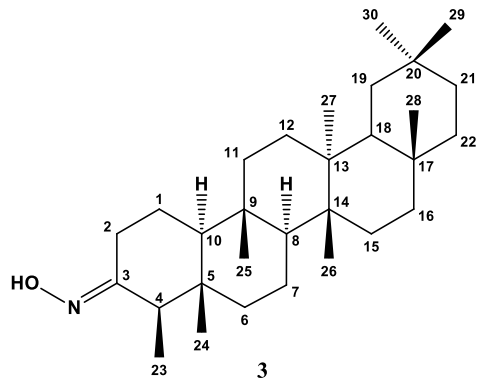


**Figure 10S.** Chemical structure of the friedelan-3-oxime derivative (3)

In the infrared spectrum of *N*-derivative **3**, absorption bands were observed at  $3300\text{ cm}^{-1}$  ( $\nu_{OH}$ ),  $2928\text{ cm}^{-1}$  ( $\nu_{CH}$ ), and at  $1450$  and  $1380\text{ cm}^{-1}$  ( $\nu_{CH}$ ), characteristic of aliphatic compounds. A broad

absorption band at  $3300\text{ cm}^{-1}$  ( $\nu_{\text{N-OH}}$ ) and intense absorption at  $960\text{ cm}^{-1}$  characterized the presence of the oxime group.<sup>1</sup> In the  $^1\text{H}$  NMR spectrum, a quartet was observed at  $\delta_{\text{H}} 3.75$  associated with the H-4 characteristic of triterpenes of the friedelane series.<sup>2</sup> The doublet at  $\delta_{\text{H}} 3.65$  was associated with H-2 (axial). A signal was also detected at  $\delta_{\text{H}} 3.51$ , attributed to the hydrogen oxime group. In the  $^{13}\text{C}$  NMR spectrum, the signal at  $\delta_{\text{C}} 160.00$  was assigned to carbon C-3 (Figures 11S to 15S).

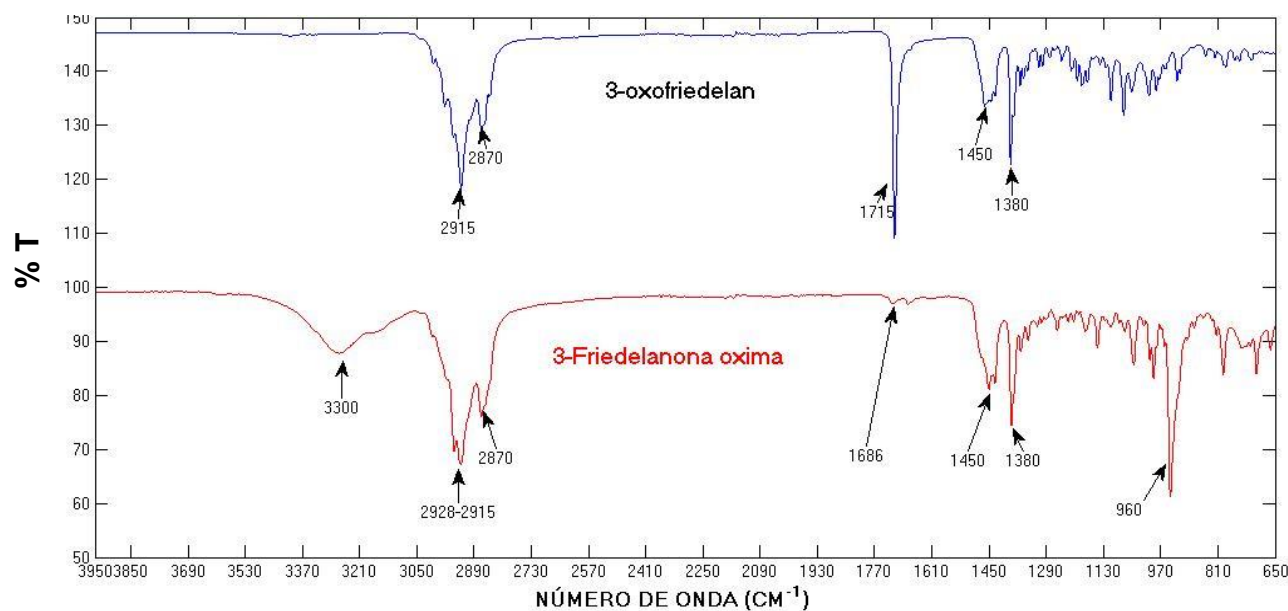


**Figure 11S.** IR spectrum (ATR) of friedelan-3-oxime (3) compared to friedelin (3-oxo-friedelan)

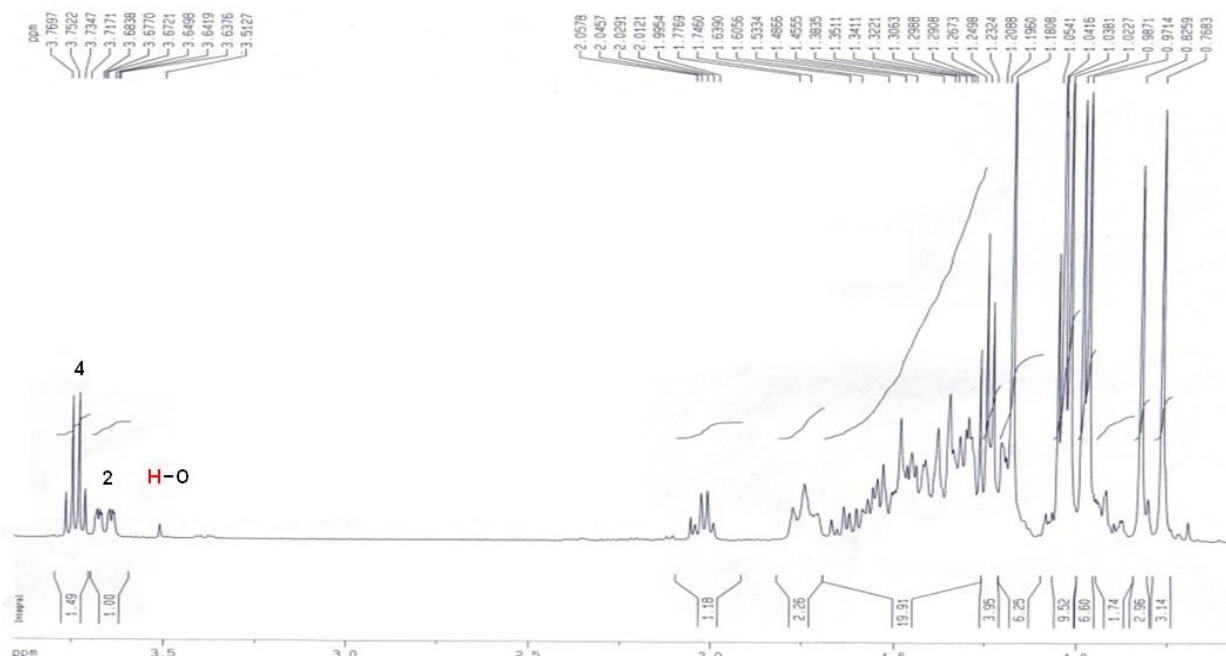


**Figure 12S.**  $^1\text{H}$  NMR spectrum (400 MHz,  $\text{CDCl}_3/\text{pyridine}-d_5$ ) of friedelan-3-oxime (3)

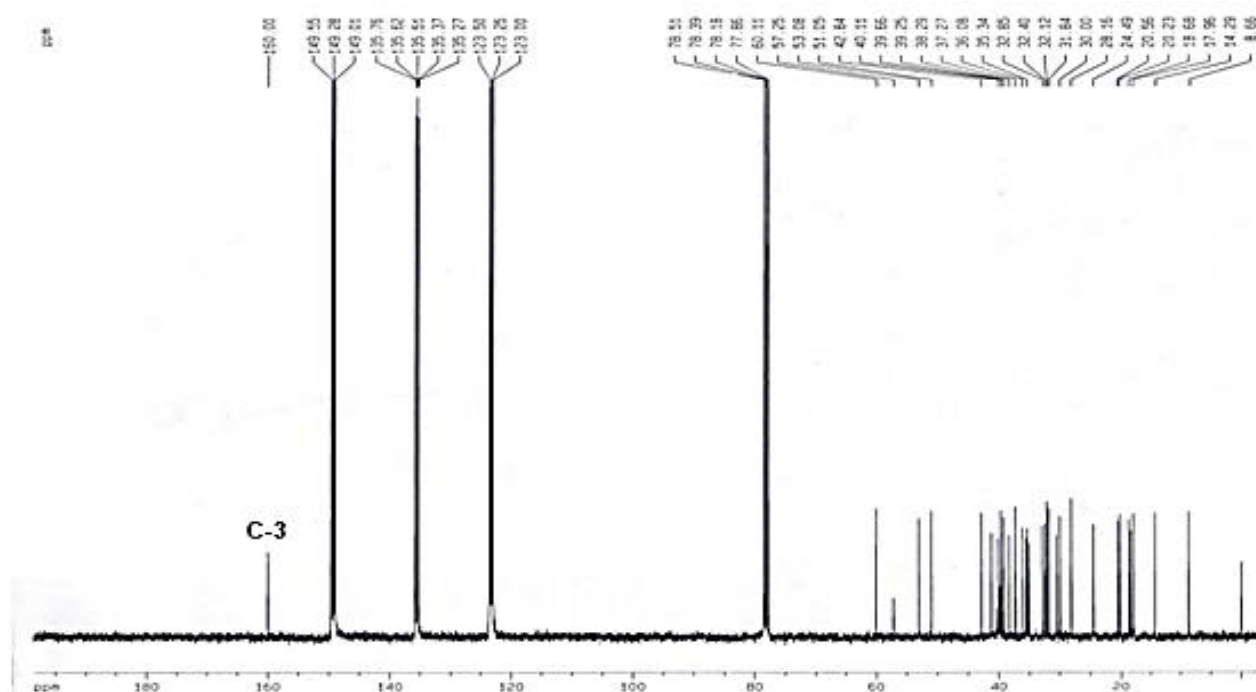


**Figure 13S.**  $^{13}\text{C}$  NMR spectrum (100 MHz,  $\text{CDCl}_3/\text{pyridine-}d_5$ ) of friedelan-3-oxime (3)

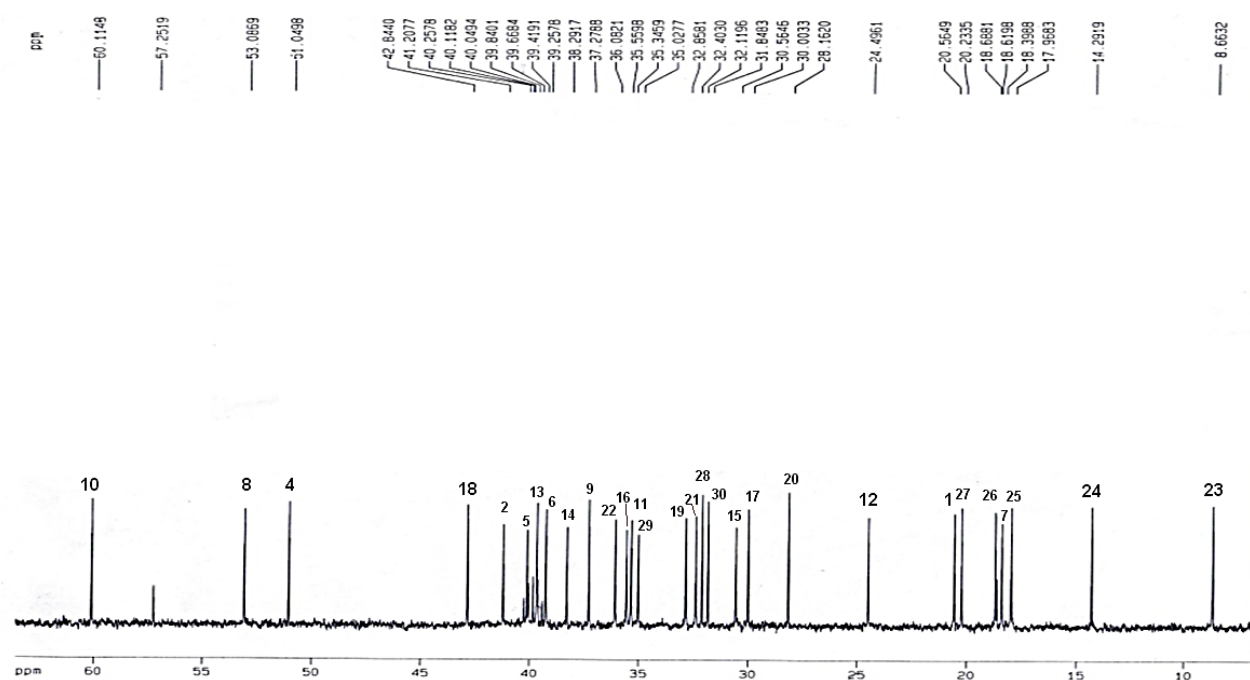


**Figure 14S.**  $^{13}\text{C}$  NMR spectrum (100 MHz,  $\text{CDCl}_3/\text{pyridine-}d_5$ ) of friedelan-3-oxime (**3**). Expansion between  $\delta_{\text{C}}$  7.00 and 64.00 ppm

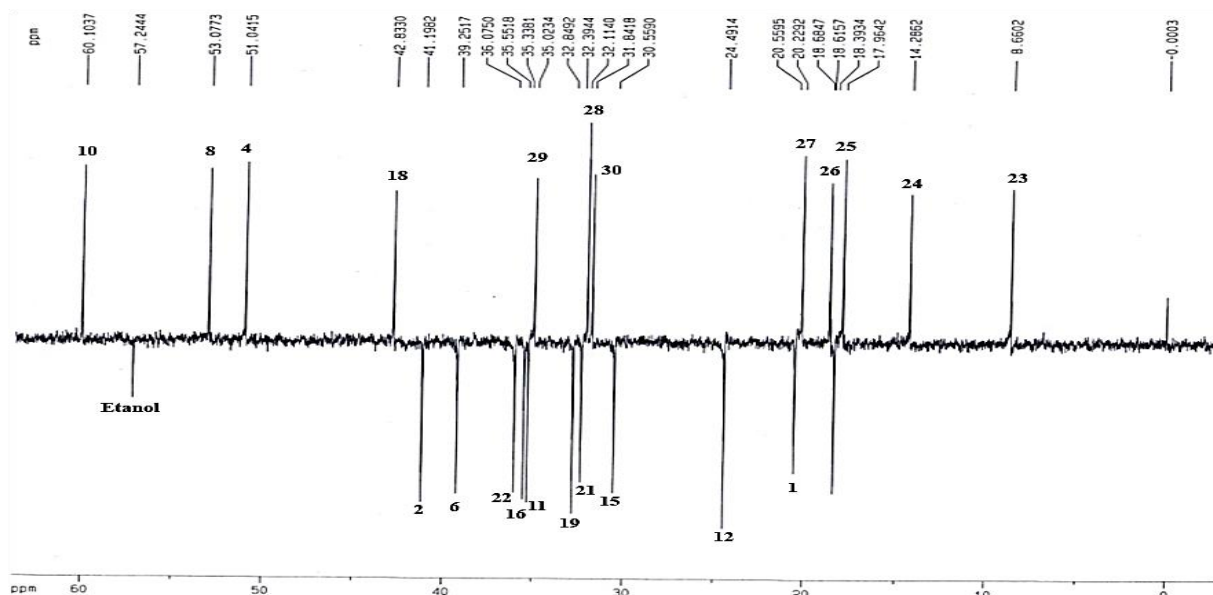


**Figure 15S.** DEPT-135 spectrum (100 MHz,  $\text{CDCl}_3/\text{pyridine-}d_5$ ) of friedelan-3-oxime (3)

#### Spectral data of friedelan-3-hydrazone (4)

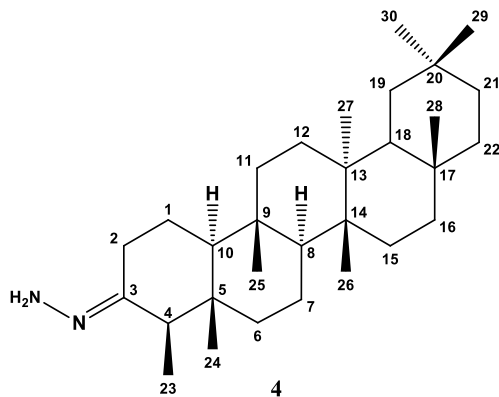


**Figure 16S.** Chemical structure of the friedelan-3-hydrazone derivative (4)

In the spectrum of *N*-derivative 4, the absorption bands at 2915 and 2860  $\text{cm}^{-1}$  ( $\nu_{\text{CH}}$ ) and 1450 and 1380  $\text{cm}^{-1}$  ( $\delta_{\text{CH}}$ ) correlated with the aliphatic compounds C–H bond.<sup>1</sup> In the  $^1\text{H}$  NMR spectrum, the multiplet at  $\delta_{\text{H}} 5.30$  was attributed to the hydrogen bonded to the nitrogen of the hydrazone group.<sup>2</sup> The signal at  $\delta_{\text{C}} 172.92$  observed in the  $^{13}\text{C}$  NMR spectrum was attributed to C-3 (Figures 17S to 20S).

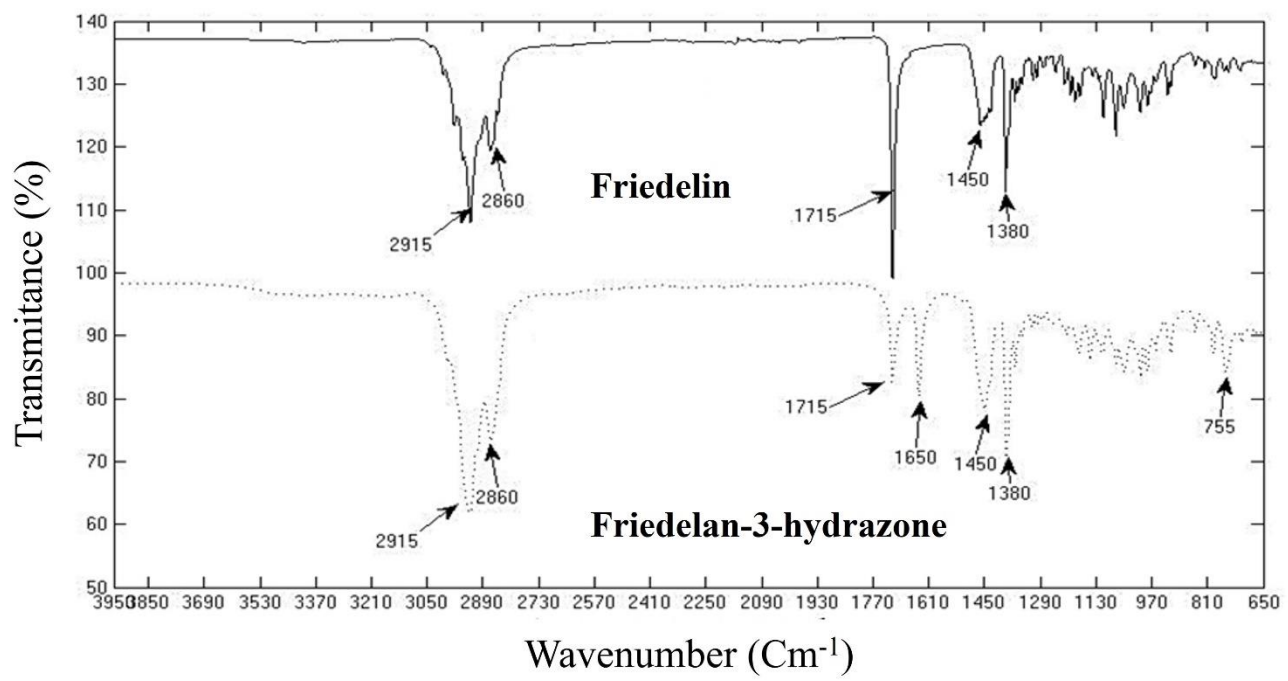


**Figure 17S.** IR spectrum (ATR) of friedelan-3-hydrazone (**4**) compared to friedelin (**1**)

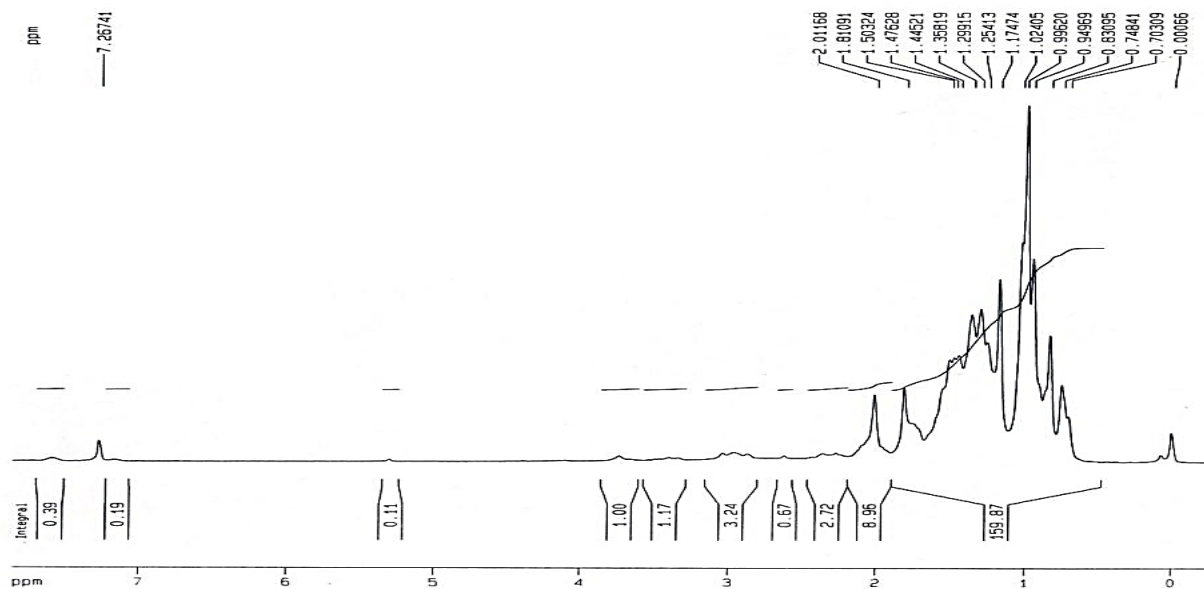


**Figure 18S.** <sup>1</sup>H NMR spectrum (400 MHz, CDCl<sub>3</sub>) of friedelan-3-hydrazone (**4**)

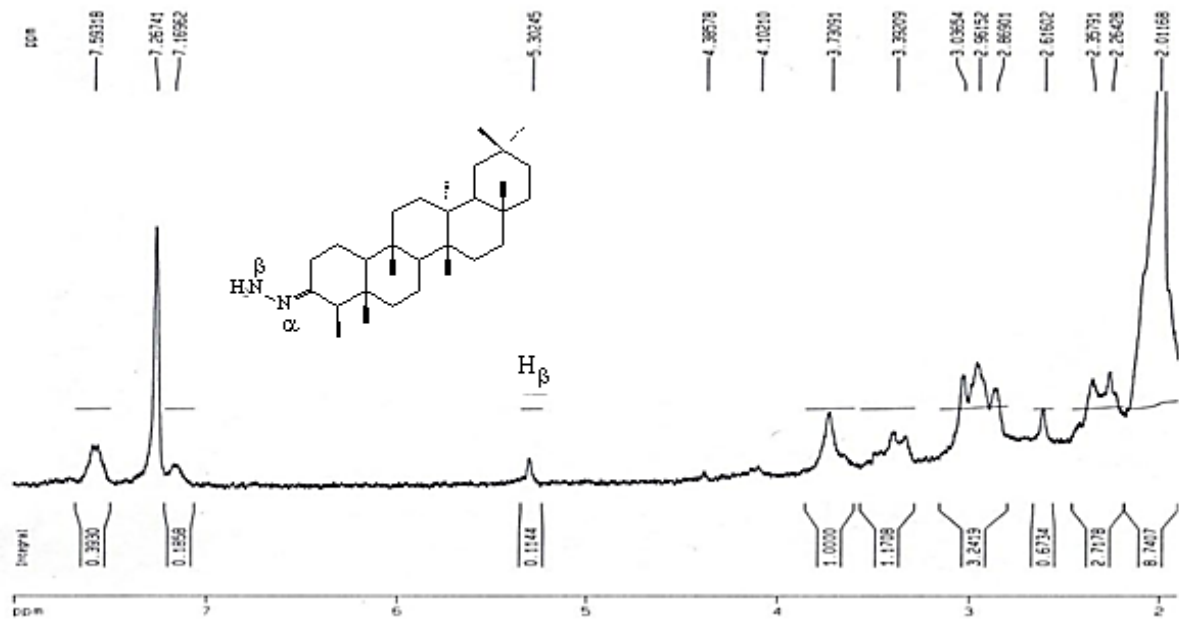


**Figure 19S.**  $^1\text{H}$  NMR spectrum (400 MHz,  $\text{CDCl}_3$ ) of friedelan-3-hydrazone (**4**). Expansion between  $\delta_{\text{H}}$  2.00 to 8.00 ppm

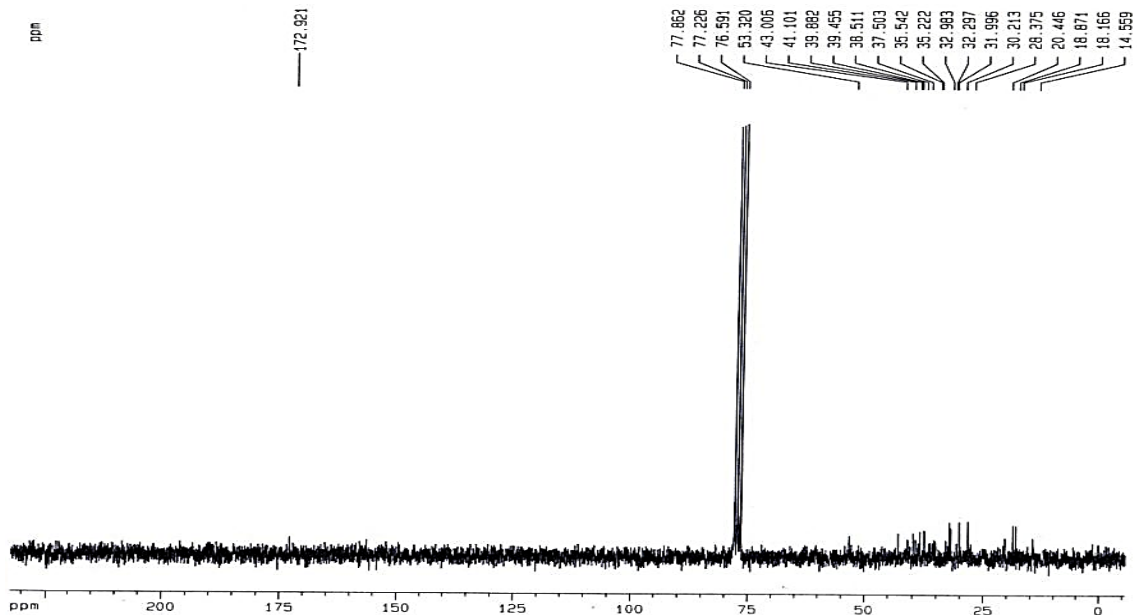


**Figure 20S.**  $^{13}\text{C}$  NMR spectrum (100 MHz,  $\text{CDCl}_3$ ) of friedelan-3-hydrazone (**4**)

The  $^{13}\text{C}$  NMR data including DEPT-135 of friedelan-3-(2,4-dinitrophenylhydrazone) (**2**), friedelan-3-oxime (**3**) and friedelan-3-hydrazone (**4**) derivatives are shown in Table 2S.

**Table 2S.**  $^{13}\text{C}$  NMR data including DEPT-135 of friedelan-3-(2,4-dinitrophenylhydrazone) (**2**), friedelan-3-oxime (**3**) and friedelan-3-hydrazone (**4**) derivatives from friedelin isolated from *Maytenus gonoclada*

Carbon	Friedelin <i>N</i> -derivatives					
	<b>2</b>		<b>3</b>		<b>4</b>	
	$^{13}\text{C}$ ( $\delta_{\text{C}}$ / ppm)	DEPT-135	$^{13}\text{C}$ ( $\delta_{\text{C}}$ / ppm)	DEPT-135	$^{13}\text{C}$ ( $\delta_{\text{C}}$ / ppm)	DEPT-135
1	21.32	CH <sub>2</sub>	20.56	CH <sub>2</sub>	20.86	CH <sub>2</sub>
2	41.34	CH <sub>2</sub>	36.08	CH <sub>2</sub>	41.16	CH <sub>2</sub>
3	162.62	C=N	160.00	C=NOH	172.92	C=NNH <sub>2</sub>
4	53.31	CH	51.05	CH	53.32	CH
5	41.19	C	41.20	C	41.10	C
6	36.03	CH <sub>2</sub>	39.84	CH <sub>2</sub>	35.79	CH <sub>2</sub>
7	18.37	CH <sub>2</sub>	18.39	CH <sub>2</sub>	18.58	CH <sub>2</sub>
8	53.11	CH	53.09	CH	52.84	CH
9	37.41	C	37.28	C	37.50	C
10	59.88	CH	60.11	CH	60.39	CH
11	35.36	CH <sub>2</sub>	35.34	CH <sub>2</sub>	35.54	CH <sub>2</sub>
12	27.25	CH <sub>2</sub>	24.49	CH <sub>2</sub>	28.37	CH <sub>2</sub>
13	38.34	C	40.26	C	38.51	C
14	39.27	C	38.29	C	39.46	C
15	32.42	CH <sub>2</sub>	30.55	CH <sub>2</sub>	32.60	CH <sub>2</sub>
16	35.36	CH <sub>2</sub>	35.56	CH <sub>2</sub>	35.22	CH <sub>2</sub>
17	30.03	C	30.00	C	30.75	C
18	41.19	CH	42.84	CH	43.00	CH
19	32.80	CH <sub>2</sub>	36.08	CH <sub>2</sub>	32.98	CH <sub>2</sub>
20	28.18	C	28.16	C	30.21	C
21	35.60	CH <sub>2</sub>	32.85	CH <sub>2</sub>	35.77	CH <sub>2</sub>
22	30.51	CH <sub>2</sub>	39.25	CH <sub>2</sub>	30.72	CH <sub>2</sub>
23	8.77	CH <sub>3</sub>	8.66	CH <sub>3</sub>	8.90	CH <sub>3</sub>
24	14.40	CH <sub>3</sub>	14.29	CH <sub>3</sub>	14.56	CH <sub>3</sub>
25	17.96	CH <sub>3</sub>	17.97	CH <sub>3</sub>	18.17	CH <sub>3</sub>
26	18.67	CH <sub>3</sub>	20.23	CH <sub>3</sub>	18.88	CH <sub>3</sub>
27	20.24	CH <sub>3</sub>	18.68	CH <sub>3</sub>	20.45	CH <sub>3</sub>

**Table 2S.**  $^{13}\text{C}$  NMR data including DEPT-135 of friedelan-3-(2,4-dinitrophenylhydrazone) (**2**), friedelan-3-oxime (**3**) and friedelan-3-hydrazone (**4**) derivatives from friedelin isolated from *Maytenus gonoclada* (cont.)

Carbon	Friedelin <i>N</i> -derivatives					
	<b>2</b>		<b>3</b>		<b>4</b>	
	$^{13}\text{C}$ ( $\delta_{\text{C}}$ / ppm)	DEPT-135	$^{13}\text{C}$ ( $\delta_{\text{C}}$ / ppm)	DEPT-135	$^{13}\text{C}$ ( $\delta_{\text{C}}$ / ppm)	DEPT-135
28	31.80	CH <sub>3</sub>	32.11	CH <sub>3</sub>	31.99	CH <sub>3</sub>
29	35.03	CH <sub>3</sub>	35.03	CH <sub>3</sub>	35.03	CH <sub>3</sub>
30	32.11	CH <sub>3</sub>	31.84	CH <sub>3</sub>	32.30	CH <sub>3</sub>
1'	145.69	aromatic ring	—	—	—	—
2'	116.45	aromatic ring	—	—	—	—
3'	123.64	aromatic ring	—	—	—	—
4'	137.40	aromatic ring	—	—	—	—
5'	129.96	aromatic ring	—	—	—	—
6'	128.79	aromatic ring	—	—	—	—

—: absence of the carbon corresponding to the specified number.

## PART B - MODELING ANTILEISHMANIAL ACTIVITY

### The process used to build the Leishmania Modeled Datasets

A search for “*Leishmania*” in PubChem Bioassay yielded 11,515 assays. A manual filtering process eliminated 5,970 that were not related to parasites of the *Leishmania* family. Another 992 bioassays that addressed toxicity (cytotoxicity, renal and hepatic toxicity, etc.), selectivity index, anti-inflammatory, and immunological effects were also eliminated. Ultimately, 4,553 assays were classified according to the specific species, the infecting forms (amastigotes, promastigotes, and macrophages), and the specific biological targets. Bioassays containing too many compounds were eliminated:

AID: 1721: qHTS Assay for Inhibitors of *Leishmania Mexicana* Pyruvate Kinase (LmPK)

Protein Target: pyruvate kinase

Substance BioActivity: 1089 Active, 16 Activity  $\leq 1 \mu\text{M}$ , 293196 Tested

AID: 1722: qHTS Assay for Activators of *Leishmania Mexicana* Pyruvate Kinase (LmPK)

Protein Target: pyruvate kinase

Substance BioActivity: 16 Activity  $\leq 1 \mu\text{M}$ , 293196 Tested

AID: 1063: *Leishmania major* promastigote HTS

Substance BioActivity: 17630 Active, 196173 Tested

AID: 1671155: *Leishmania* intramacrophage assay

Substance BioActivity: 34 Active, 68614 Tested

AID: 1671175: *Leishmania infantum* Histidine tRNA synthetase (LdHisRS)

Protein Target: Histidine tRNA synthetase

Substance BioActivity: 75 Active, 8 Activity  $\leq 1 \mu\text{M}$ , 68613 Tested

The files containing the raw bioassay data for each one were downloaded from PubChem in CSV format (“Complete Data Table”). 526 CSV files were unavailable, and only 1498 bioassays contained substances classified (“PUBCHEM\_ACTIVITY\_OUTCOME”) as active or inactive. Hence, these datasets were grouped according to the classification (infecting forms and specific targets) and used to build the corresponding models. The compounds in each group of bioassays were analyzed for redundancy, inconsistencies, and access to the 3D structures on the PubChem Compounds website. In the end, from the total of 45 possible datasets, only 10 viable datasets were obtained, which meet the conditions for model construction (a minimum of 15 active and 15 inactive compounds). Their compositions are presented in Tables 3S-5S, shown below.

## The composition of *Leishmania* datasets and modeling results

**Table 3S.** Modeled datasets associated with *Leishmania* species, infecting forms, or specific targets. Include the total of unique bioassays (according to PubChem Bioassay identifier – AID) and the number of compounds in each dataset

Model	<i>Leishmania</i> Species	Infecting form or target	Number of bioassays (AID)	Number of compounds
LBP	<i>L. braziliensis</i>	promastigote	32	109
LDP	<i>L. donovani</i>	promastigote	261	955
LAA	<i>L. amazonensis</i>	amastigote	73	236
LDA	<i>L. donovani</i>	amastigote	272	2727
LIA	<i>L. infantum</i>	amastigote	78	600
LIP	<i>L. infantum</i>	promastigote	97	233
LMjP	<i>L. major</i>	promastigote	96	1431
LMxP	<i>L. mexicana</i>	promastigote	20	84
LMjPR	<i>L. major</i>	pteridine reductase 1	18	111
LMxPK	<i>L. mexicana</i>	pyruvate_kinase	7	1453

**Table 4S.** Modeled datasets associated with *Leishmania* species, infecting forms, or specific targets. Include the number of compounds (according to PubChem Compound identifier – CID) classified as active or inactive in the OUTCOME field of PubChem Bioassay tables. The values of the area under the ROC curve (AUC<sub>ROC</sub>) obtained from the SVM and Naïve Bayes modeling processes are also shown

Model	Dataset	Number of	Number of	AUC	AUC
		active CID	inactive CID	SVM	Bayes
LBP	<i>L. braziliensis</i> promastigote	73	36	0.932	0.868
LDP	<i>L. donovani</i> promastigote	684	271	0.913	0.810
LAA	<i>L. amazonensis</i> amastigote	182	54	0.970	0.969
LDA	<i>L. donovani</i> amastigote	1532	1195	0.990	0.947
LIA	<i>L. infantum</i> amastigote	472	128	0.961	0.929
LIP	<i>L. infantum</i> promastigote	179	54	0.933	0.905
LMjP	<i>L. major</i> promastigote	409	1022	0.788	0.751
LMxP	<i>L. mexicana</i> promastigote	51	33	0.984	0.999
LMjPR	<i>L. major</i> pteridine reductase 1	37	74	0.915	0.769
LMxPK	<i>L. mexicana</i> pyruvate kinase	95	1358	0.958	0.873

**Table 5S.** List of Pubchem Bioassay identifiers (AID) used to build the *Leishmania* datasets modeled in this work

Model	Dataset	Total AID	List of AIDs
LBP	<i>L. braziliensis</i> promastigote	32	332682 332674 332675 332679 332676 1417105 597220
			445552 313537 1484680 416456 1517529 1517538
			380082 1429969 1176089 472708 452946 768746
			1645894 771991 1569852 612696 612698 756038 537134
			336635 336636 1054904 396585 396616 265561
LDP	<i>L. donovani</i> promastigote	261	1699392 1143756 659704 292979 292983 1226080
			1061073 1260577 1184287 1695402 1594994 1698020
			1698021 1166652 1548455 1740565 1548456 1740566
			1517477 1853812 1766401 1766403 1304621 1456714
			397821 270072 427813 427814 427811 1711511 313538
			412471 1812213 1528609 1685489 604069 668283
			1740558 1742367 1196492 1690284 416314 416310
			416311 416307 416313 416309 416312 416308 1426547
			1426562 1524588 420955 1599205 1599203 1360068
			1411450 1609652 1599196 1599198 1599200 1599199
			1695403 456123 1493777 486920 431404 487936
			1484690 1627864 1699384 1550486 1601777 1601776
			701538 321798 1487717 332683 332688 332680 332677
			660299 458966 669325 1723644 261353 459128 607446
			284258 322584 339570 1077515 453388 346549 1514103
			1093457 1093663 1384264 282105 456796 1292207
			346048 346049 346050 346051 1778832 1699388
			1699391 1699390 1699389 1118189 284383 1387670
			355991 1564991 1564986 1550491 533171 533172
			533170 533173 1564996 1564990 1547479 1299437
			647778 1415705 1778827 1778826 1850391 1646239
			1085764 1517426 707359 707362 1115389 1679091
			1236506 1186380 1632241 768743 1728581 744548
			1307134 1257056 754989 1678975 1360423 1360424
			1595001 1586945 1194918 1406965 1609645 1609646
			1464424 1359723 1359726 1079677 1288817 1272824
			549914 515927 747506 1699380 1225360 1548454
			1740564 1514109 1766395 1360422 1699381 1586979
			1406970 1167551 780211 1143801 780199 703487

			1181720 1181722 514352 703620 703621 346053
			1120597 101042 1077476 279546 294358 336634 336395
			336394 710593 27157 267789 95931 95929 303682
			100144 325357 100415 1550500 1389735 1389733
			1389734 1426642 1426641 1426640 1426639 1599258
			1599259 1778851 1778860 1778850 1599264 1599262
			1550494 1550493 1609703 1609701 1609702 1564995
			1564992 1599263 1550502 1550501 1550497 1550503
			1550504 710585 1138741 707370 707368 707372
			1599248 1550492 1564994 1699393 1699396 1850400
			1850399 1226085 100414 252067 396584 396615
			1318777 757796 1204248 303680 710586 279036 279037
			279034 279035 1586980 1586981 1406972 1406971
			100430
<hr/>			
			283867 1243754 1243753 1243747 1243748 1243750
			1243749 1180419 1755647 1191158 1394817 1394842
			1255051 1294729 1518062 1695401 1695399 1154488
			533155 1766398 1829961 1829962 1829963 1829964
			1829966 1829965 1829956 1829960 1365597 1365624
LAA	<i>L. amazonensis</i>	73	636858 421916 256083 1254991 1254987 472707 452950
	amastigote		1545098 1484707 412472 1417132 1604175 1395336
			472705 452945 549987 1514128 1395333 1604177
			1432297 1382410 1493782 1847231 1550662 396588
			396618 1352647 1352642 1335348 1304623 1514521
			1514519 1697058 99843 1432295 1400239 95769
			1318781 733445 609556 1054892 1243756 1420627
<hr/>			
			595217 595220 1176208 659708 707361 707360 1115388
			1249022 1547541 1336588 1267132 494333 1755656
			1290502 1290480 754985 1260578 723305 723304
			754988 1290451 1894825 1078195 1233220 1678916
LDA	<i>L. donovani</i>	272	1778829 1778828 1175543 1056392 1359732 1595000
	amastigote		768742 746921 579905 747505 765720 1699383 1764057
			1267127 1318791 1254918 744547 1300854 1299434
			1078098 536812 1113804 607316 1299551 419757
			314662 1174773 1138744 1174775 1464425 1586949
			1184284 1331513 1184291 1154487 1194921 1061072
			533154 533157 1406967 487938 487935 1426583

---

		1426584 1426593 1426594 1426595 1426596 731442
		352870 352869 1395340 1417116 455184 458967
		1592313 1468880 1164986 1858984 1468873 272979
		1695409 1695406 1699387 1166653 1660997 1483100
		696205 1813886 766604 526299 1514104 308328
		1571822 1571821 267787 311527 311646 315955 533153
		419681 453256 612453 1491573 361583 1862835
		1491574 1491577 338404 338403 1439216 1395339
		463748 389016 1384266 1384265 1546408 1456713
		1456711 439583 1468959 1564985 1279257 1277389
		1571547 1317213 1652801 1571548 1468867 1417122
		1741959 1713385 1355405 1586760 1405622 1504890
		372585 1881373 668285 1230467 1426548 1426545
		1426546 1426563 1484694 1468958 1599206 1599204
		1599197 1599195 1599202 1609648 1599201 1360069
		1411451 696372 696208 776400 776398 1360072 468176
		1278522 776408 387299 1250475 1778834 1778833
		1501096 486921 431406 431405 392000 391999 1395338
		312854 1270040 1194730 432047 701537 1638411
		389454 346042 431463 1399458 1399459 1399454
		1468961 378965 1432880 1657542 1505032 677565
		315107 632298 1639466 1653751 1653743 1649501
		1270041 1328471 1181721 703479 780200 762342
		439874 780204 779141 703486 626318 1165092 1245582
		515985 346922 1394864 1460819 1460815 1460814
		1460820 1394866 1460817 727319 1462700 303264
		1410116 1455942 774779 562113 1614007 644367
		418752 1177052 1177056 1240906 710594 303246
		430071 748435 1336582 100282 685532 1336584 113843
		140476 113844 100145 100146 279027 279018 1207582
		1207580 977614 255970 95922 1166658 315961 315960
		707371 95764 651891 651892 310825 100421 100412
		255960 100424 248971 252048
LIA	<i>L. infantum</i> amastigote	295906 1180422 1695292 1695290 1695291 1695289
		1695293 1695288 1753483 1267128 493471 1755655
		1290452 1371065 1384911 1348369 1546283 1678914
		1569863 1406960 1815843 1815842 1765173 1360417

---

			502407 1569862 1228664 1569829 1167372 1167371 1879379 1868684 1766400 456124 1381692 1381689 1337422 1468874 1468881 1624266 1586950 1713260 1384261 1450422 1329378 1501881 736786 1230466 1395366 1813887 1685285 1468960 1742369 1617792 1548445 523341 1847233 321799 781030 1649505 1517423 1569865 1569864 1468962 1181716 1278150 1514508 1287596 640230 464089 1475117 744601 1868725 1868718 1318780 1359172 1585176 1054893
LIP	<i>L. infantum</i> promastigote	97	1569859 744771 744772 1879408 1879406 1879407 530576 1713264 1594997 1847204 1780640 1780630 1713259 1337421 1517484 1517485 1484691 284070 397822 1384260 1514119 1365623 454754 454753 1524589 668284 1329377 736791 1501880 1238023 1766399 1384905 1176085 456122 321797 1649502 1649537 1649538 1230480 1230479 1230493 1230492 1230484 1230483 530577 1569861 1569860 1847206 1847230 1180408 1054876 1054875 1054879 1054878 1569858 1765172 1228672 1594993 1699382 1569913 1569914 1359731 1569828 378887 1868688 1868689 1868690 780205 1181717 1335271 1278149 1162128 1514507 1094751 1094755 1094752 1094749 1094750 295904 1054880 1054877 1094754 1094753 1054905 265560 1318776 1585174 1264449 1054888 1054890 1517417 1517416 1517481 1569872 1569871 1569887 1569888
LMjP	<i>L. major</i> promastigote	96	1594998 1855169 362759 329295 466920 1698022 1847227 1185950 397823 1484676 1484675 1473364 1484699 1484700 1484689 477038 1539151 1539152 1853814 1417106 701542 1273854 678016 1510697 1517427 1358318 1434385 693605 1255035 374556 1728580 1288816 1275219 1255576 1096510 1096511 1096508 1096504 1096509 1096507 1096503 1096506 1586951 1601779 1601778 1359730 536813 1272822 747454 662818 378886 537133 586924 1484674 586925 523278 523288 523279 1143799 1233723 1674463 1260758 1492828 1188427 1079813 372446 586929

			586930 586928 587016 587015 100908 101020 310824
			248801 587019 586927 587020 587017 587018 586926
			1539162 1539161 1539157 1539158 1539159 1539156
			312863 2008 1258 1533741 1628324 372445 372444
			1204247 695815
LMxP	<i>L. mexicana</i> promastigote	20	372576 394405 1514110 532354 532356 598284 532353 532355 376976 1847236 672473 1143800 502041 514355 101021 101022 1592309 1592307 1592310 1592308
LMjPR	<i>L. major</i> pteridine reductase 1	18	1196726 1471022 1471019 1589592 1589588 554332 554321 554309 708605 1689604 1333041 444877 708405 1892320 1471020 1471021 1333047 1333045
LMxPK	<i>L. mexicana</i> pyruvate kinase	7	476346 2559 2561 1881866 2266 959 945

#### Prediction of antileishmanial activity of pentacyclic triterpenes (TTPs)

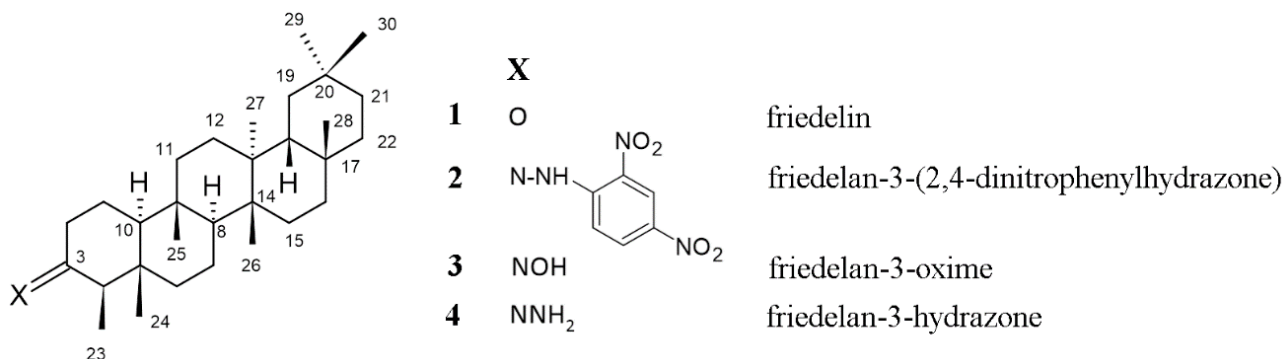


**Figure 21S.** Chemical structures of friedelin (**1**), isolated from dried leaves of *Maytenus gonoclada*, and of its N-derivatives (**2-4**)

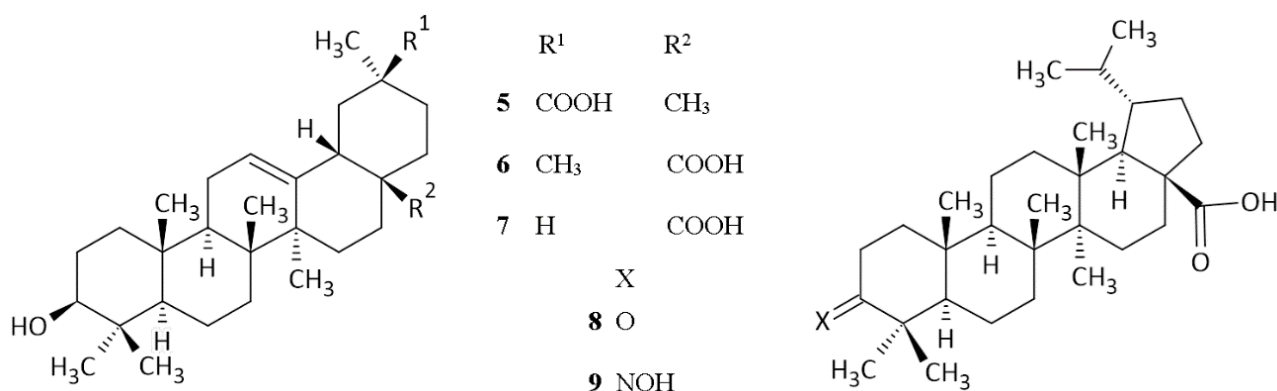


**Figure 22S.** Chemical structures of pentacyclic triterpenes with activity against *Leishmania*:  $\beta$ -glycyrrhetic acid (**5**),  $\beta$ -oleanolic acid (**7**), ursolic acid (**6**), betulonic acid (**8**), and betulonic acid oxime (**9**)

**Table 6S.** Values of Pa-Pi (probability of being active minus probability of being inactive) calculated for all compounds analyzed by SVM modeling with the Active-IT system. Bold numbers indicate values that surpass the cutoff values for SVM (Pa-Pi > 0.5)

Model	<b>1</b>	<b>2</b>	<b>3</b>	<b>4</b>	<b>5</b>	<b>6</b>	<b>7</b>	<b>8</b>	<b>9</b>
LBP	<b>0.808</b>	0.355	<b>0.795</b>	<b>0.808</b>	<b>0.753</b>	<b>0.795</b>	<b>0.808</b>	<b>0.767</b>	<b>0.767</b>
LDP	0.392	<b>1.000</b>	0.249	0.353	<b>0.540</b>	<b>0.613</b>	<b>0.544</b>	0.464	<b>0.514</b>
LAA	0.335	<b>0.989</b>	0.357	0.363	<b>0.571</b>	0.390	0.401	0.385	0.396
LDA	0.140	<b>0.667</b>	0.194	0.268	<b>0.513</b>	<b>0.537</b>	<b>0.616</b>	0.333	0.459
LIA	0.185	-0.071	0.155	0.185	0.018	0.155	0.135	0.155	0.155
LIP	0.334	-0.059	0.256	<b>0.605</b>	-0.148	-0.142	-0.148	-0.131	-0.142
LMjP	-0.065	<b>0.609</b>	-0.058	-0.164	0.498	0.148	0.298	0.045	0.241
LMxP	-0.147	0.430	-0.141	-0.111	-0.044	-0.137	-0.097	-0.137	-0.109
LMjPR	-0.676	0.297	-0.635	-0.405	-0.541	-0.689	-0.703	-0.595	-0.635
LMxPK	-0.54	-0.904	-0.483	-0.536	-0.711	-0.627	-0.714	-0.609	-0.654

LBP: *L. braziliensis* promastigote; LDP: *L. donovani* promastigote; LAA: *L. amazonensis* amastigote; LDA: *L. donovani* amastigote; LIA: *L. infantum* amastigote; LIP: *L. infantum* promastigote; LMjP: *L. major* promastigote; LMxP: *L. mexicana* promastigote; LMjPR: *L. major* pteridine reductase 1; LMxPK: *L. mexicana* pyruvate kinase.

**Table 7S.** Values of Pa-Pi (probability of being active minus probability of being inactive) calculated for all compounds analyzed by Naïve Bayes modeling with the Active-IT system. Bold numbers indicate values that surpass the cutoff values for Naïve Bayes (Pa-Pi > 0.8)

	1	2	3	4	5	6	7	8	9
LBP	<b>0.92</b>								
LDP	<b>0.84</b>								
LAA	<b>0.93</b>								
LDA	0.11	<b>0.92</b>	0.10	<b>0.92</b>	0.10	0.16	0.15	0.15	0.15
LIA	0.02	<b>1.00</b>	0.02	0.10	0.06	0.14	0.12	0.16	0.12
LIP	-0.03	-0.03	-0.03	0.13	-0.44	-0.40	-0.46	-0.30	-0.40
LMjP	0.54	0.58	0.52	0.47	0.60	0.58	0.58	0.58	0.58
LMxP	-0.07	0.01	-0.08	-0.05	-0.16	-0.15	-0.20	-0.13	-0.15
LMjPR	0.35	0.41	0.41	0.41	0.39	0.26	0.27	0.27	0.31
LMxPK	-0.53	-0.12	-0.59	-0.63	-0.84	-0.74	-0.77	-0.77	-0.78

LBP: *L. braziliensis* promastigote; LDP: *L. donovani* promastigote; LAA: *L. amazonensis* amastigote; LDA: *L. donovani* amastigote; LIA: *L. infantum* amastigote; LIP: *L. infantum* promastigote; LMjP: *L. major* promastigote; LMxP: *L. mexicana* promastigote; LMjPR: *L. major* pteridine reductase 1; LMxPK: *L. mexicana* pyruvate kinase.

**Table 8S.** Experimental inhibitory concentrations at 50% ( $IC_{50}$ ) for some pentacyclic triterpenes against promastigote forms of *Leishmania* species. Pa-Pi (probability of being active minus probability of being inactive) values are also included for *Leishmania* species for which models are available

Compound	$IC_{50}$ / $\mu M$	Pa-Pi		<i>Leishmania</i> species (promastigotes)	Reference
		SVM	Naive Bayes		
Friedelin ( <b>1</b> )	> 450	—	—	<i>L. amazonensis</i>	4
Friedelan-3-(2,4-dinitrophenylhydrazone) ( <b>2</b> )	14.67	—	—	<i>L. amazonensis</i>	this work
Friedelan-3-oxime ( <b>3</b> )	65.82	—	—	<i>L. amazonensis</i>	this work
beta-Glycyrrhetic acid ( <b>5</b> )	9.77	0.54	0.838	<i>L. donovani</i>	5
Ursolic acid ( <b>6</b> )	11 to 20	—	—	<i>L. amazonensis</i>	5-7
Oleanic acid ( <b>7</b> )	22 to 45	—	—	<i>L. amazonensis</i>	4,6,8,9
Betulonic acid ( <b>8</b> )	8.5	0.767	0.917	<i>L. braziliensis</i>	10

## REFERENCES

1. Silverstein, R. M.; Bassler, G. C.; Morrill, T. C.; *Spectrometric identification of organic compounds*, 5<sup>th</sup> ed.; Wiley: New York, 1991.
2. Agrawal, P. K.; *Phytochemistry* **1992**, *31*, 3307. [[Crossref](#)]
3. Bretmaier, E.; Voelter, W.; *Carbon-13 NMR spectroscopy*, 3<sup>rd</sup> ed.; VCH: New York, 1987.
4. Torres-Santos, E. C.; Lopes, D.; Oliveira, R. R.; Carauta, J. P.; Falcao, C. A.; Kaplan, M. A.; Rossi-Bergmann, B.; *Phytomedicine* **2004**, *11*, 114. [[Crossref](#)]
5. Ukil, A.; Biswas, A.; Das, T.; Das, P. K.; *J. Immunol.* **2005**, *175*, 1161. [[Crossref](#)]
6. Gnoatto, S. C.; Dalla Vechia, L.; Lencina, C. L.; Dassonville-Klimpt, A.; Da Nascimento, S.; Mossalayi, D.; Guillou, J.; Gosmann, G.; Sonnet, P.; *J. Enzyme Inhib. Med. Chem.* **2008**, *23*, 604. [[Crossref](#)]
7. Yamamoto, E. S.; Campos, B. L.; Jesus, J. A.; Laurenti, M. D.; Ribeiro, S. P.; Kallás, E. G.; Rafael-Fernandes, M.; Santos-Gomes, G.; Silva, M. S.; Sessa, D. P.; Lago, J. H. G.; Levy, D.; Passero, L. F. D.; *PloS ONE* **2015**, *10*, e0144946. [[Crossref](#)]
8. Melo, T. S.; Gattass, C. R.; Soares, D. C.; Cunha, M. R.; Ferreira, C.; Tavares, M. T.; Saraiva, E.; Parise-Filho, R.; Braden, H.; Delorenzi, J. C.; *Parasitol. Int.* **2016**, *65*, 227. [[Crossref](#)]

9. Sifaoui, I.; López-Arencibia, A.; Martín-Navarro, C. M.; Ticona, J. C.; Reyes-Batlle, M.; Mejri, M.; Jiménez, A. I.; Lopez-Bazzocchi, I.; Valladares, B.; Lorenzo-Morales, J.; Abderabba, M.; Piñero, J. E.; *Phytomedicine* **2014**, *21*, 1689. [[Crossref](#)]
10. Alcazar, W.; López, A. S.; Alakurtti, S.; Tuononen, M.-L.; Yli-Kauhaluoma, J.; Ponte-Sucre, A.; *Bioorg. Med. Chem.* **2014**, *22*, 6220. [[Crossref](#)]



This is an open-access article distributed under the terms of the Creative Commons Attribution Licence.